Food and Bioprocess Technology
https://doi.org/10.1007/s11947-018-2083-8

ORIGINAL PAPER

Rheological and Microstructural Characterization of Wheat Dough Formulated with High Levels of Resistant Starch

Carlos Gabriel Arp[1] · María Jimena Correa[1] · Cristina Ferrero[1]

Received: 31 October 2017 / Accepted: 14 February 2018

Abstract

Fiber-enriched breads can contribute to increasing the daily fiber intake. Resistant starches (RS) are a useful resource to increase the amount of non-digestible carbohydrates while preserving as far as possible the technological quality of white bread. The effects of high concentrations of Hi-Maize (HM), a type 2 RS, in dough formulations were analyzed by farinograph, dynamic rheometric assays, texture profile analysis, and ^{1}H-NMR relaxation measurements and related to particle size and microstructural characteristics studied by different microscopy techniques (SEM, ESEM, CLSM). Up to 30% replacement with HM was performed. Water absorption increased and development time and stability decreased when the amount of HM increased. Water mobility increased suggesting a change in water binding. The mechanical spectra indicated a prevalence of the solid-like character in all samples, but the G' (storage modulus) vs. G'' (loss modulus) plot suggested a pronounced change in the microstructure of dough at the highest level of replacement. Dough was harder, more adhesive, and less resilient when the HM content was increased. The use of HM in the premix formulations not only diluted the gluten content but also changed the size particle distribution of starch granules by increasing the fraction with smaller sizes. Thus, more compact matrices were obtained with a noticeable disruption of the gluten network at the highest level of replacement. However, an intermediate level of RS addition (20%) still rendered a dough with satisfactory rheological properties for breadmaking.

Keywords Wheat dough · Rheology · Resistant maize starch type 2 · Microstructure · Microscopy

Introduction

Starches are one of the main sources of energy in the human diet around the world. This vegetal component is present in the majority of foods, either as part of the ingredients of a meal or as an additive in processed foods. The selection and/or modification of different starches has been investigated to meet the requirements of many industrial applications, such as high or low viscosity, solubility in cold or hot water, high or low clarity, reduced syneresis, higher or lower gelatinization temperatures, acid resistance, as well as nutritional and healthy aspects (Singh et al. 2007).

Asp (1992) defined resistant starch (RS) as the starch and its degradation products that resist the digestion in the small intestine of healthy humans. Further investigations in the field of the mechanics of enzyme resistance have led to the classification of RS into five types: RS1–RS5 (Hasjim et al. 2013; Nugent 2005). RS1 and RS2 occur naturally in fresh foods, in vegetal structures that hinder the action of α-amylases in the former or the compact crystalline structure that prevents the enzyme access to the granule in the latter. RS3 is a thermally modified starch whose crystalline structure is enhanced by retrogradation becoming also compact and resistant, RS4 is a chemically modified starch, and in RS5 the amylose-lipid complex reduces starch availability. There are also many studies about the healthy properties of RS, specifically regarding its low glycemic index and its prebiotic effects when it acts as dietary fiber (Alfa et al. 2017; Fuentes-Zaragoza et al. 2010; Grabitske and Slavin 2009; Keenan et al. 2006; Scholz-Ahrens et al. 2007; Topping et al. 2003).

Thus, the incorporation of resistant starches in foods of good acceptance and accessibility is increasingly becoming a good strategy aiming to the rise in dietary fiber consumption. In fact, RS are used in many cereal food systems such as breakfast cereals and nutrition bars (Aigster et al. 2011; Brennan et al. 2008), gluten-free products (Korus et al.

✉ Cristina Ferrero
cferrero@biol.unlp.edu.ar

[1] Centro de Investigación y Desarrollo en Criotecnología de Alimentos (CIDCA) (Universidad Nacional de La Plata-Facultad de Ciencias Exactas, Comisión de Investigaciones Científicas de la Provincia de Buenos Aires, Consejo Nacional de Investigaciones Científicas y Técnicas), 47 y 116 (C.P 1900), La Plata, Argentina

Published online: 06 March 2018

2009; Tsatsaragkou et al. 2015), pasta (Aravind et al. 2013; Bustos et al. 2011), breads and baked goods (Almeida et al. 2013a, b; Baixauli et al. 2008; Yeo and Seib 2009). In addition, efforts have been made to improve the quality of breads formulated with RS type 2 (RS2) using enzymes and emulsifiers such as transglutaminase, glucose oxidase, DATEM, SSL, and PS80 (Altuna et al. 2015, 2016; Sanchez et al. 2014). However, there is a lack of knowledge about the effect of RS2 concentration on the microstructure of white bread doughs.

It is known that the rheological behavior of dough is a determinant factor during kneading, loaf shaping, leavening, and the final loaf expansion in the oven. At the same time, the rheological behavior of dough is closely related to its microstructure and the interactions among components. So, a more thorough comprehension about the relationship between rheology and structure can contribute to improve the formulation of premixes to obtain composite breads.

The aim of this work was to study the effect of high concentrations of RS2 on white bread dough formulations by fundamental and empirical rheology and microscopic characterization. The partial substitution methodology was employed in order to evaluate doughs prepared with different concentrations of RS2 in contrast with non-RS2 dough (control).

Materials and Methods

Materials

Commercial wheat flour (WF) (Molino Campodónico, Argentina), Hi-Maize260™ resistant corn starch (HM) (Ingredion Inc., USA), and NaCl (Celusal, Argentina) were used for the preparation of dough samples. WF alveographic characteristics were $P = 121$ mmH_2O, $L = 85$ mm, $P/L = 1.42$, and $W = 390 \times 10^{-4}$ J. HM is a RS2, containing 60% (dry basis) of insoluble dietary fiber in the form of resistant starch.

Formulation of the Premixes

Premix samples were prepared by replacing WF with HM in different proportions, with a NaCl constant level of 2% (*w*/*w* (WF basis or WF/HM mix basis, as appropriate)). Substitution levels of WF for HM were 0, 10, 20, and 30% (control, HM10, HM20, and HM30, respectively). Premixes moisture values were between 13.0% (control) and 11.3% (HM30).

Farinograms

The resistance of doughs to mixing was assayed in a Brabender farinograph (Duisburg, Germany) with mixing bowl for 300 g of flour. Wheat flour, WF with NaCl, and mixes of WF/NaCl/HM were assessed at 30 ± 0.2°C in duplicate according to a modification of the constant flour weight (variable dough weight) AACC 54-21.01 procedure (AACC International 2000a). The modification consisted in the addition of NaCl (2%) to wheat flour and premixes as is described in Arp et al. (2017). In order to characterize the mixing properties of the samples, the following parameters were extracted from the farinograms: water absorption (WA), development time (DT), stability (S), and degree of softening (DS). WA is defined as the percentage of water to reach a consistency of 500 BU (Barabender Units); development time is the time necessary to reach up to 500 BU; stability is the time that dough remains at a consistency of 500 BU, and degree of softening is defined as the difference in BU from middle curve at peak to middle curve measured at 12 min after peak is reached. The determination was done in duplicate.

Solvent Retention Capacity

The solvent retention capacity of WF and premixes (prepared without NaCl) was determined according to AACC 56-11.02 procedure (AACC International 2000b). Water, sucrose (50%, *w*/*w*), sodium carbonate (5%, *w*/*w*), and lactic acid (5%, *w*/*w*) retention capacities (WaRC, SuRC, SCRC, and LARC, respectively) were evaluated for each sample. Briefly, the method consists in the addition of each solvent (25 ml) to premixes (5 g) which are allowed to solvate and swell (20 min). Then, samples are centrifuged (1000×*g*; 15 min) and the supernatant is discarded. The amount of solvent retained by each sample is determined by weight (gel wt). The solvent retention capacity (SRC) values were calculated by Eq. 1.

$$\mathrm{SRC} = \left\lfloor \frac{\text{gel wt}}{\text{premix wt}} \right\rfloor \times \left\lfloor \frac{86}{100 - \text{flour moisture}} \right\rfloor \times 100 \quad (1)$$

where premix wt means premix weight.

Also, the gluten performance index (GPI) was calculated as GPI = LARC / (SuRC + SCRC) (Kweon et al. 2011). The assay was performed at least in duplicate.

Starch Granule Sizing by Laser Diffraction

Starch granules from HM and WF were measured with a Mastersizer 2000E (Malvern Instruments Ltd., UK) in order to quantify the particle size. Starch granules from WF were previously extracted. The extraction of WF starch was done by collecting the washing volume from dough samples during gluten determination. The washing volume was left to dry at room temperature by placing it as a thin layer on a plastic support. Starches were suspended in distilled water (10%, *w*/*w*) prior to the size measurement. Approximately 1 ml of each suspension was added to the stirred water bath and then passed

through the equipment measuring system. Refractive indexes of 1.33 and 1.52 for water and starch, respectively, were used. Obscuration ranged from 12 to 14% for all the measurements. The starch granule size was evaluated in terms of the 10th percentile ($D(0.1)$), the 50th percentile or median ($D(0.5)$), the 90th percentile ($D(0.9)$), the volume moment mean ($D[4,3]$), and the specific surface area, which were obtained from the volume weighted distribution. The determination was done at least in duplicate.

Preparation of Dough Samples

Dough samples were prepared using a planetary kneader (Kenwood, Italy). The premixes were dry-mixed at the lowest speed (52 rpm) in the kneader bowl for 60 s. For each premix, the farinographic parameter WA was taken as the optimum amount of water to be added, and the parameter DT was employed as kneading time. Water was added at the first minute of kneading, and then the speed was increased to 89 rpm until completing the kneading time. Once kneaded, doughs were allowed to rest for 10 min prior to any assay. For each formulation, two independent doughs were prepared.

Moisture Content and Water Activity

Approximately 3 g of each dough sample was weighed to 0.0001 g precision for the determination of the moisture content by weight loss in a gravity convection oven (San Jor, Argentine) at 105 °C for 24 h. All determinations were done in triplicate for each dough replicate.

The evaluation of water activity (a_w) was performed at 25 °C in an AquaLab Series 4 (Decagon Devices Inc., USA) using plastic cups to place the samples. Pieces of dough big enough to completely cover the plastic cup base were assessed in triplicate for each dough replicate.

Determination of Gluten Content

Values of wet and dry gluten for WF and premixes were obtained with a Glutomatic 2200 (Perten Instruments, Sweden). The assays were performed according to Correa et al. (2010), which involved the preparation of the dough as was described previously outside the mixing/washing chamber of the Glutomatic. Then, 15.0 ± 0.1 g of the dough was placed in the Glutomatic chamber for the washing process according to the original method. The determination was performed at least in duplicate for each dough replicate.

Small Amplitude Oscillatory Test

After the kneading, doughs were covered with a plastic film to avoid dehydration and were allowed to rest for 10 min at room temperature. For the assessment, dough was laminated (2 mm height) and cylindrical pieces of 3 cm diameter were obtained by means of a rounded cutter. The doughs were evaluated in a Haake RS600 rheometer (Thermo Science, Germany) equipped with a serrated parallel plate system of 30 mm diameter. A gap of 1.5 mm between plates was used. A stress sweep protocol was performed for the determination of the linear viscoelastic range (LVR) of the doughs. Four cylindrical pieces were subjected to increasing oscillation amplitudes from 0.5 to 200 Pa at a constant frequency of 1 Hz. Once the LVR was determined, six cylindrical pieces for each dough were assessed in a frequency sweep protocol from 0.005 to 100 Hz at a constant stress of 5 Pa (within the LVR) in order to obtain the mechanical spectra. Before the beginning of each assay, all samples were covered with liquid Vaseline oil to avoid dough dehydration and allowed to rest for 15 min in the measurement position for their relaxation and thermostatization at 25 °C. The values of storage modulus (G'), loss modulus (G''), and tangent of phase angle (tan δ) were analyzed. Both moduli were fitted to a logarithmic linearized power law equation (Eqs. 2 and 3)

$$\log G'(\omega) = \log a + n \log \omega \quad (2)$$

$$\log G''(\omega) = \log b + m \log \omega \quad (3)$$

where ω is the frequency in hertz, $\log a$ and $\log b$ are the intercept at $\omega = 0$ Hz, and n and m are the slopes of the curves.

Texture Profile Analysis

For texture assay, dough samples were sheeted to 1 cm height and cut into small cylindrical pieces by means of a stainless steel round cutter. These pieces were covered by a film from the moment they were cut until they were measured to avoid sample dehydration. Dough pieces were subjected to two consecutive cycles of compression until 40% of their height with a P/75 probe (75 mm diameter) in a TA.XT2i Texture Analyzer (Stable Micro Systems, UK) that was placed in a room at constant temperature (25 °C). The parameters of hardness, consistency, cohesiveness, adhesiveness, springiness, resilience, and gumminess were extracted from the resulting texture profile analysis (TPA). For each formulation, a total of 32 dough pieces from two independent dough samples were assessed.

^{1}H-NMR Relaxation Measurements

Spin-spin ^{1}H relaxation times (T_2) were determined with a low-resolution MiniSpec pc120 spectrometer (Bruker, Germany) using Carr–Purcell–Meiboom–Gill (CPMG) sequence with an interpulse spacing of 200 μs. For this purpose, doughs were prepared in duplicate, and each duplicate was measured in three different NMR tubes. Also, each tube was

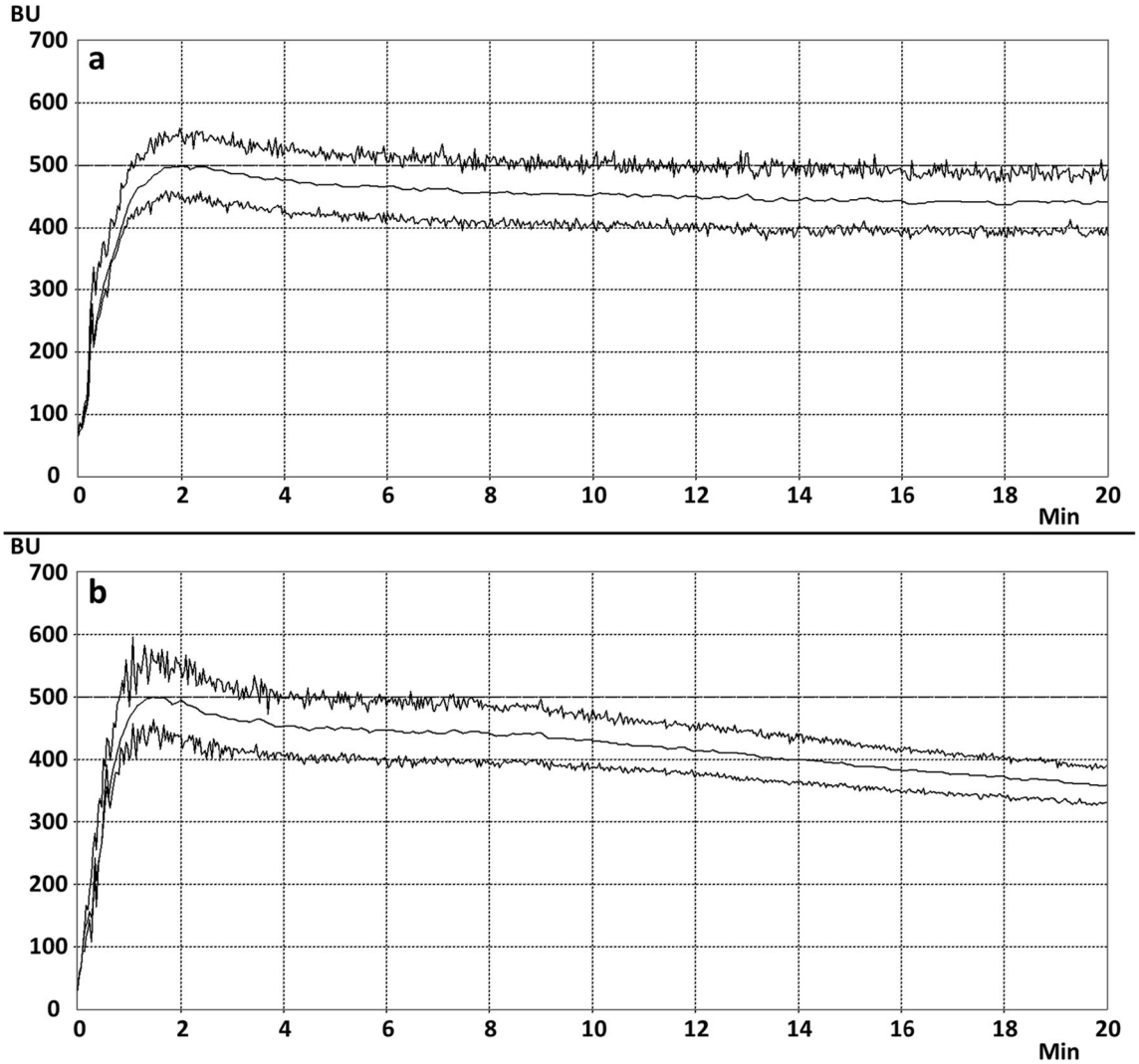

Fig. 1 Farinograms of the control (**a**) and HM30 premix (**b**)

measured in triplicate, rotating it 90° between consecutive measurements. Tubes were prepared by placing portions of dough and compressing it using a glass plunger.

Scanning Electron Microscopy

The fracture surface of dehydrated doughs was observed in a Jeol JSM-6360 LV (Japan) scanning electron microscope (SEM). The preparation of the doughs required first an immersion in glutaraldehyde (2.5%, *v*/*v*) for fixation, second, a progressive dehydration of the fixated doughs with acetone aqueous solutions at increasing concentrations: 0, 25, 50, 75, and 100% (*v*/*v*), washing the doughs three times for 5 min with each solution. Once the third washing with acetone 100% (*v*/*v*) was done, samples were placed in a Baltec CPD30 (Liechtenstein) critical point dryer for the complete dehydration of the doughs. Then, samples were metallized with gold using a Jeol Fine Coat Ion Sputter JFC1100 (Japan). The samples were then ready for observation. Micrographs of different fields were acquired at 300×.

Environmental Scanning Electron Microscopy

The samples of doughs were mounted onto a support for observation in an FEI Quanta 200 environmental scanning electron microscope (ESEM), at 4.14 Torr atmospheric pressure and 10 °C. Micrographs of different fields were acquired at 1000×. Micrographs were acquired at "Servicio de Microscopía Electrónica y Microanálisis (SeMFi-LIMF)—Facultad de Ingeniería, UNLP, Argentina."

Confocal Scanning Laser Microscopy

Samples of dough slices were non-covalently dyed with an aqueous solution of rhodamine B (0.001%, *w*/*v*), fluorescein isothiocyanate (FITC) (0.01% (*w*/*v*) in $NaHCO_3$ 0.005 mM and NaCl 0.01 mM, pH 9) for 60 min in dark conditions. Then, all samples

Table 1 Farinographic parameters for wheat flour (WF) and premixes with different levels of substitution

	WA (ml)	DT (min)	S (min)	DS (BU)
WF	58.8 ± 0.3 b	9.8 ± 1.3 b	21.0 ± 0.9 c	32 ± 6 a
Control	55.4 ± 0.8 a	9.8 ± 1.4 b	30.0 ± 3.2 d	19 ± 8 a
HM10	58.2 ± 0.2 b	8.6 ± 1.6 ab	22.3 ± 1.7 c	30 ± 1 a
HM20	60.3 ± 0.3 c	6.8 ± 0.2 a	15.8 ± 1.7 b	57 ± 13 b
HM30	63.1 ± 0.4 d	6.7 ± 0.2 a	12.2 ± 0.4 a	85 ± 11 c

Mean values ± standard deviation. Different letters in the same column indicate statistical differences ($p < 0.05$; $n = 2$)

Control, HM10, HM20, and HM30, premixes with substitution levels of WF for resistant starch of 0, 10, 20, and 30%, respectively; WA, water absorption; DT, development time; S, stability; DS, degree of softening; BU, Brabender units

were observed with an Olympus FV1000 confocal microscope. The excitation wavelengths were 568 and 488 nm, and the emission wavelengths were 625 and 518 nm for rhodamine B and FITC, respectively. Micrographs were taken at 20×.

The digital images obtained were analyzed with ImageJ 1.49p software (National Institutes of Health, USA) in order to quantify the complexity of the protein matrix. For this purpose, rhodamine B channel micrographs were selected due to a more suitable representation of the protein network than the one acquired with the FITC channel. An FFT filtering process was applied to images for shading and smoothing correction of artifacts. Then, the Otsu's algorithm was used to binarize structures. The Fractal Box Count tool was used for counting the number (N) of r-size boxes needed to fill the structures. The fractal dimension (FD) of the matrix was then calculated using the following equation:

$$N(r) = k \times r^{-\mathrm{FD}} \tag{4}$$

where k is a constant.

Statistical Analysis

The one-way ANOVA and Fisher LSD tests for determination of statistically different means at a level of 0.05 were performed on OriginPro 8 SR0 v8.0724 (USA). The Pearson's correlation analysis was done employing the Statgraphics Centurion XV v15.2.06 software (StatPoint Inc.) at 95% confidence level.

Results and Discussion

Solvent Retention Capacity, Mixing Properties, and Gluten Values of Wheat Flour and Premixes

Representative farinograms of the control and HM30 samples are shown in Fig. 1. In general, qualitative and quantitative differences were found in the farinograms of the control and mixes with HM. The ones corresponding to samples with HM showed a pronounced peak of consistency at the beginning of the curve that was not present in the control sample. This peak would be related to rapid water absorption by starch granules, so samples with more relative amount of starch (mixes with HM) presented a more pronounced peak. The same effect was previously observed in mixes of wheat flour and chemically modified resistant starch (Arp et al. 2017). Table 1 lists the farinographic parameters of WF and premixes. The parameters extracted from farinograms showed that when NaCl (2%, *w*/*w*) is added to WF, a reduction in WA and DS and a marked increase in S occurs. This effect has been associated with an increase of cross-linking in the gluten network when NaCl is present (Ukai et al. 2008).

Table 2 Solvent retention capacity (SRC) and gluten determination of premixes

	WF	HM10	HM20	HM30
WaRC[a]	66.9 ± 0.6 a	68.0 ± 1.0 b	68.5 ± 0.9 b	70.2 ± 0.2 c
SuRC[a]	110.4 ± 2.3 c	107.0 ± 2.0 b	103.6 ± 2.2 a	101.7 ± 1.3 a
SCRC[a]	82.1 ± 0.9 a	81.3 ± 0.6 a	81.6 ± 0.7 a	82.0 ± 0.5 a
LARC[a]	107.3 ± 1.4 d	100.4 ± 1.5 c	90.6 ± 0.8 b	86.0 ± 0.60 a
GPI	0.557 ± 0.010 d	0.533 ± 0.007 c	0.489 ± 0.006 b	0.468 ± 0.005 a
Wet gluten (WG)[b]	21.4 ± 0.4 d	19.8 ± 0.6 c	17.2 ± 0.5 b	16.1 ± 0.5 a
Dry gluten (DG)[b]	7.2 ± 0.1 d	6.7 ± 0.4 c	5.8 ± 0.2 b	5.5 ± 0.3 a
WG/DG	3.0 ± 0.1	3.0 ± 0.2	3.0 ± 0.1	2.9 ± 0.2
WG-DG[b]	14.2 ± 0.6	13.1 ± 0.7	11.4 ± 0.7	10.6 ± 0.6

Different letters in the same row indicate statistical differences

WaRC, water retention capacity; SuRC, sucrose retention capacity; SCRC, sodium carbonate retention capacity; LARC, lactic acid retention capacity; GPI, gluten performance index

[a] Values expressed as % *w*/*w* (dry basis). Samples prepared without NaCl. Mean values ± standard deviation ($p < 0.05$; $n = 2$)

[b] Values expressed as % *w*/*w*. Mean values ± standard deviation ($p < 0.05$; $n = 8$)

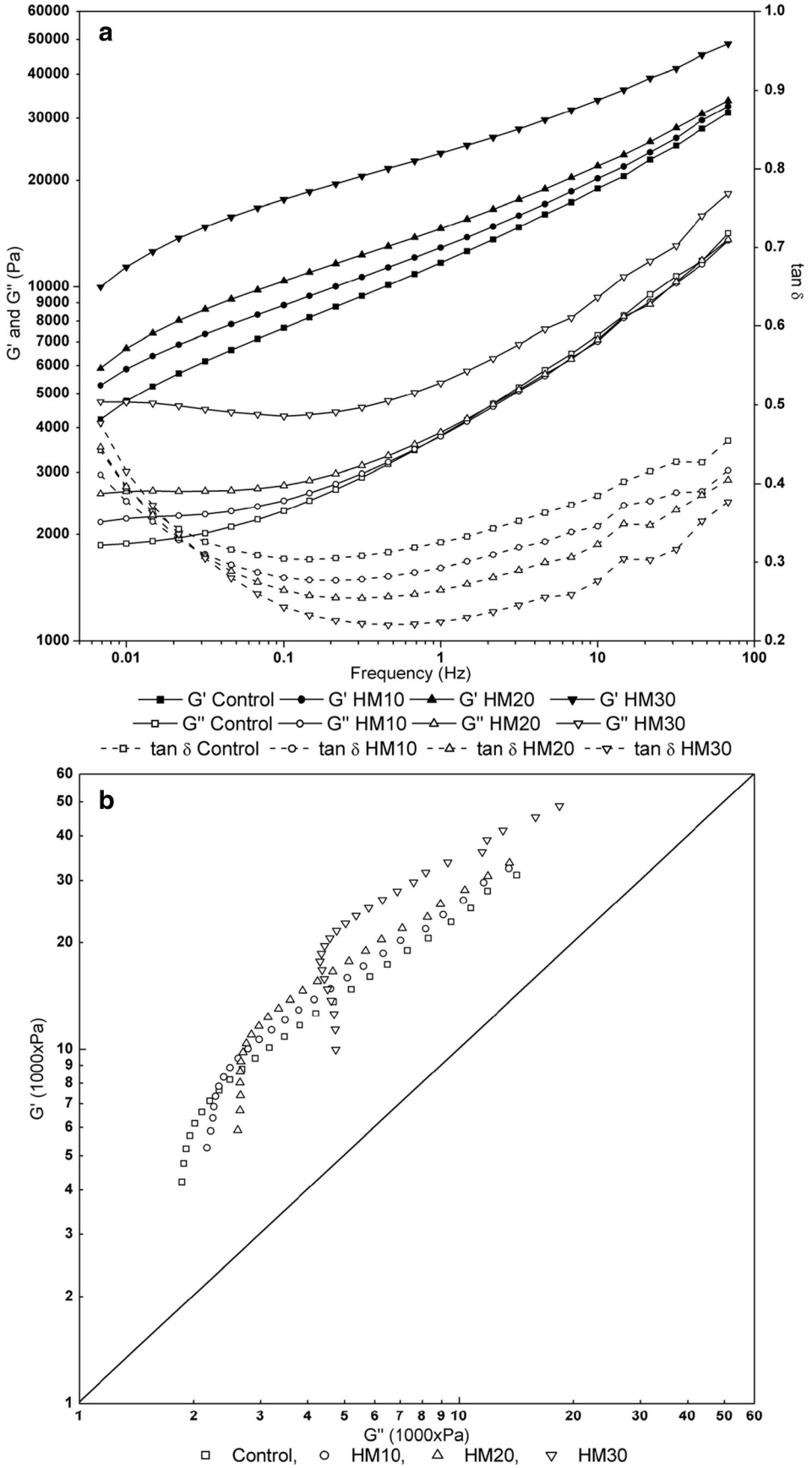

Fig. 2 Small amplitude oscillatory rheology of doughs. **a** Mechanical spectra showing G', G'', and tan δ; **b** G' vs. G'' plot

When increasing levels of HM were added, a progressive increase in WA was observed.

On the other hand, the stabilizing effect of NaCl gradually reverted when increasing amounts of HM were used, as shown by the decreasing values of S and increasing values of DS. Finally, a reduction of DT was observed when HM was used, especially for high levels of replacement. These changes can be mainly attributed to a dilution effect on gluten network due to the addition of the starch. The consequent diminution in gluten proportion and network quality is reflected in dough behavior during kneading. Several authors have reported this effect in different systems containing non-wheat flours or starches (Dhingra and Jood, 2004; Sabanis and Tzia 2009; Bigne et al. 2016).

The SRC and gluten values of the control sample and mixes are given in Table 2. The SRC test is a solvation assay based on the enhanced swelling behavior of individual polymer networks of wheat flour in selected solvents. This test is used to predict the functional contribution of gluten, damaged starch, and arabinoxylans to overall flour water absorption. The gluten performance index (GPI) was calculated from SRC values. GPI has been proposed as a better predictor of the overall performance of flour glutenins (Kweon et al. 2011). An increase in water absorption (WaRC) with the increase in the amount of HM was observed, while LARC (related to glutenins hydration) and SuRC (related to fiber water absorption) decreased. Concomitantly, GPI showed a progressive reduction. These effects can be associated with gluten proteins and pentosans dilution when WF is replaced by HM. However, the value of SCRC (associated with damaged starch) did not exhibit any significant changes between samples.

Table 2 shows that wet and dry gluten values decreased with HM concentration, as expected due to the dilution effect, which causes a concomitant decrease in the amount of water found in wet gluten (WG-DG). However, the WG/DG ratio remains constant in all samples (ca. three times their own dry weight). This would suggest that the water absorption capacity of gluten proteins would not be significantly affected by the substitution with HM.

Rheology of Doughs

The LVR and the mechanical spectra of doughs were obtained. In the case of LVR experiments, it was found that all samples were independent of both the storage and loss moduli with the shear stress until values near 7 Pa. In all cases, the curve for G' was higher than the one for G'' in the entire shear range, and both presented a progressive displacement to higher values at increasing levels of replacement (data not shown).

The mechanical spectra were obtained at a constant shear stress of 5 Pa (within the LVR) and are shown in Fig. 2a. Storage moduli were always above the respective loss moduli, thus indicating a predominance of the solid-like character.

G' could be adjusted to Eq. 2 in the entire range of frequencies ($r^2 \geq 0.9776$). In the case of G'', the adjustment to the power law (Eq. 3) was performed in the $\omega \geq 1$ Hz range of frequency ($r^2 \geq 0.9324$), due to the non-linear behavior observed at lower frequencies. The parameters obtained are listed in Table 3. A decrease in the slope was seen for G' at increasing concentration of HM, as well as a displacement of the curve at higher values, as can be deducted by the increase in log a. The decrease in the slope with increasing quantities of fiber was previously reported by Ahmed et al. (2013), and this behavior has been related to the higher solid-like properties of dough, since samples with a zero slope in the power law model are considered as true gels. For G'', only HM30 shifted to higher values, as indicated by log b. No differences were found in the slope for G''.

A G' vs. G'' plot was also built in order to analyze microstructural differences between samples (Fig. 2b). The curves for the control, HM10, and HM20 overlap, which is indicative of similar microstructural characteristics, as reported by Ahmed et al. (2013) and Salinas et al. (2015). However, HM30 presented a displacement to higher values of both G' and G'' and its plot was not overlapped with the others. This

Table 3 Regression parameters for mechanical spectra and G' vs. G'' plot (Fig. 2a, b)

	G' vs. ω		G'' vs. ω		G' vs. G''	
	log (a (Pa))	n (Pa Hz^{-1})	log (b (Pa))	m (Pa Hz^{-1})	Intercept	Slope
Control	4.07 ± 0.06 a	0.217 ± 0.004 d	3.55 ± 0.06 a	0.320 ± 0.009 a	1.4 ± 0.1 a	0.74 ± 0.03 c
HM10	4.12 ± 0.04 ab	0.200 ± 0.005 c	3.55 ± 0.04 a	0.313 ± 0.007 a	1.5 ± 0.2 a	0.73 ± 0.04 c
HM20	4.17 ± 0.04 b	0.182 ± 0.004 b	3.55 ± 0.04 a	0.313 ± 0.005 a	1.8 ± 0.1 b	0.66 ± 0.02 b
HM30	4.38 ± 0.05 c	0.157 ± 0.003 a	3.68 ± 0.04 b	0.310 ± 0.014 a	2.3 ± 0.1 c	0.57 ± 0.03 a

Mean ± standard deviation. Different letters in the same column indicate statistical differences ($p < 0.05$, $n = 6$)

ω, frequency; log a and log b, intercepts at $\omega = 0$ Hz; n and m, respective slopes; Control, HM10, HM20, and HM30, premixes with substitution levels of WF for resistant starch of 0, 10, 20, and 30%, respectively

Table 4 TPA parameters of doughs

	Control	HM10	HM20	HM30
Hardness (N)	1.3 ± 0.2 a	1.4 ± 0.3 a	1.6 ± 0.4 b	2.0 ± 0.3 c
Consistency (N s)	8.4 ± 0.9 a	8.2 ± 1.2 a	9.1 ± 1.3 b	9.9 ± 1.1 c
Cohesiveness (−)	0.75 ± 0.02 b	0.74 ± 0.02 a	0.74 ± 0.02 a	0.74 ± 0.02 a
Adhesiveness (N s)	3.5 ± 0.5 a	3.6 ± 0.6 a	4.5 ± 0.7 b	4.5 ± 0.6 b
Springiness (−)	0.92 ± 0.01 a	0.91 ± 0.01 a	0.91 ± 0.02 a	0.94 ± 0.01 b
Resilience (−)	0.076 ± 0.009 d	0.070 ± 0.008 c	0.061 ± 0.008 b	0.054 ± 0.009 a
Gumminess (N)	1.0 ± 0.2 a	1.0 ± 0.2 a	1.2 ± 0.3 b	1.5 ± 0.3 c

Mean values ± standard deviation. Different letters in the same row indicate statistical differences ($p < 0.05$, $n = 32$)

Control, HM10, HM20, and HM30, premixes with substitution levels of WF for resistant starch of 0, 10, 20, and 30%, respectively

behavior would indicate that the HM30 dough matrix has different microstructural characteristics. The curves were also fitted to the linearized power law using the values of G' and G'' at $\omega \geq 1$ Hz ($r^2 \geq 0.9523$) (Table 3). The intercept and slope values suggest that both HM20 and HM30 present differences in matrix microstructure with respect to the control and HM10, the effect being more marked in HM30.

Genovese (2012) described the filler-matrix composite model in which particles (the filler), modeled as viscoelastic spheres, fill a continuous, isotropic, and viscoelastic matrix. The rheologic effect of the filler in this system is the reinforcement of the elastic modulus, since particles act as a solid load, and the increase of the viscous modulus due to dissipation processes by friction between particles. This "solid load effect" can be clearly observed in Fig. 2a where greater G' values are obtained at higher replacements with HM in all the frequency range. Particularly, the HM30 dough exhibits the highest increment in solid behavior, probably because the matrix structure has drastically changed, as was also suggested by the farinograph results obtained in the present work. At this replacement level, the gluten network seems greatly affected.

Furthermore, based on the above conception the different behavior of G'' at low and high frequencies could be explained by the greater interactions among the dough components. At low frequencies, the rheology is governed mainly by the particle-particle interactions. Under these conditions, the friction between particles would be responsible for an additional dissipation of energy that would lead to the increase in loss modulus at increasing levels of filler (HM). Instead, at higher frequencies the particle-matrix interactions are dominant (Rueda et al. 2016). This could explain the scarce difference in G'' curves among the control, HM10, and HM20. However, since HM30 is a highly filled matrix, the friction phenomena in this sample would be enhanced, leading to the shift of G'' over all the frequency range with respect to the less filled ones.

The filler-matrix composite model could then explain the marked increase in G', the behavior at different frequencies of G'', and the microstructural changes observed for HM30 with respect to the other samples.

Texture Profile Analysis

The texture profile of the doughs was analyzed (Table 4). An increase in hardness and consistency was found when HM was used at substitution levels higher than 20%. This is in agreement with the increase in G' and could be related to the increased number of solid particles in the dough (starch

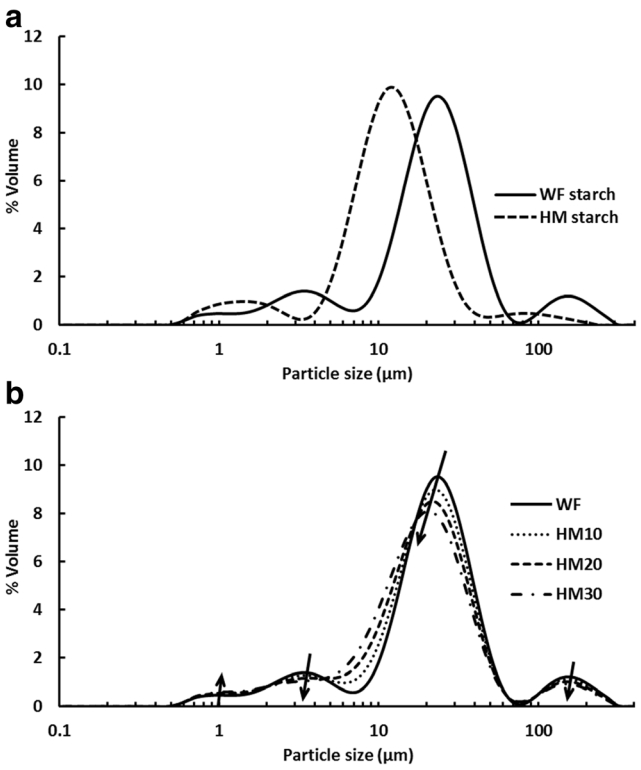

Fig. 3 Particle size distributions. **a** Percent volume for WF and HM; **b** percent volume for WF and premixes. Distributions for premixes were calculated theoretically using the WF and HM profiles. Arrows indicate the direction of the change in the peaks

Table 5 Particle size parameters

	D[4,3] (μm)	Percentiles			Specific surface area (m^2/m^3)
		D(0.1) (μm)	*D*(0.5) (μm)	*D*(0.9) (μm)	
WF	30.5 ± 0.4	3.646 ± 0.025	20.56 ± 0.07	46.00 ± 1.13	0.677 ± 0.004
HM	14.7 ± 0.1	4.263 ± 0.004	10.95 ± 0.01	22.98 ± 0.05	0.969 ± 0.000
HM10[a]	28.9 ± 0.4	3.708 ± 0.025	19.60 ± 0.07	43.70 ± 1.14	0.706 ± 0.004
HM20[a]	27.3 ± 0.4	3.769 ± 0.026	18.64 ± 0.07	41.40 ± 1.15	0.735 ± 0.004
HM30[a]	25.8 ± 0.4	3.831 ± 0.026	17.68 ± 0.07	39.09 ± 1.18	0.765 ± 0.004

D[4,3], volume moment mean; *D*(0.1), *D*(0.5), and *D*(0.9), 10th percentile, 50th percentile or median, and 90th percentile; Control, HM10, HM20, and HM30, premixes with substitution levels of WF for resistant starch of 0, 10, 20, and 30%, respectively

[a] Values for the premixes were obtained theoretically

granules). Dough adhesiveness also increased when levels of 20 and 30% of HM were employed, probably because the decrease in protein amount and poorer development of gluten network led to less bound water. Though the values for cohesiveness and springiness showed statistical differences, they were all very similar. On the other hand, the values for resilience decreased progressively with the increase in HM concentration, indicating a diminished instant elasticity

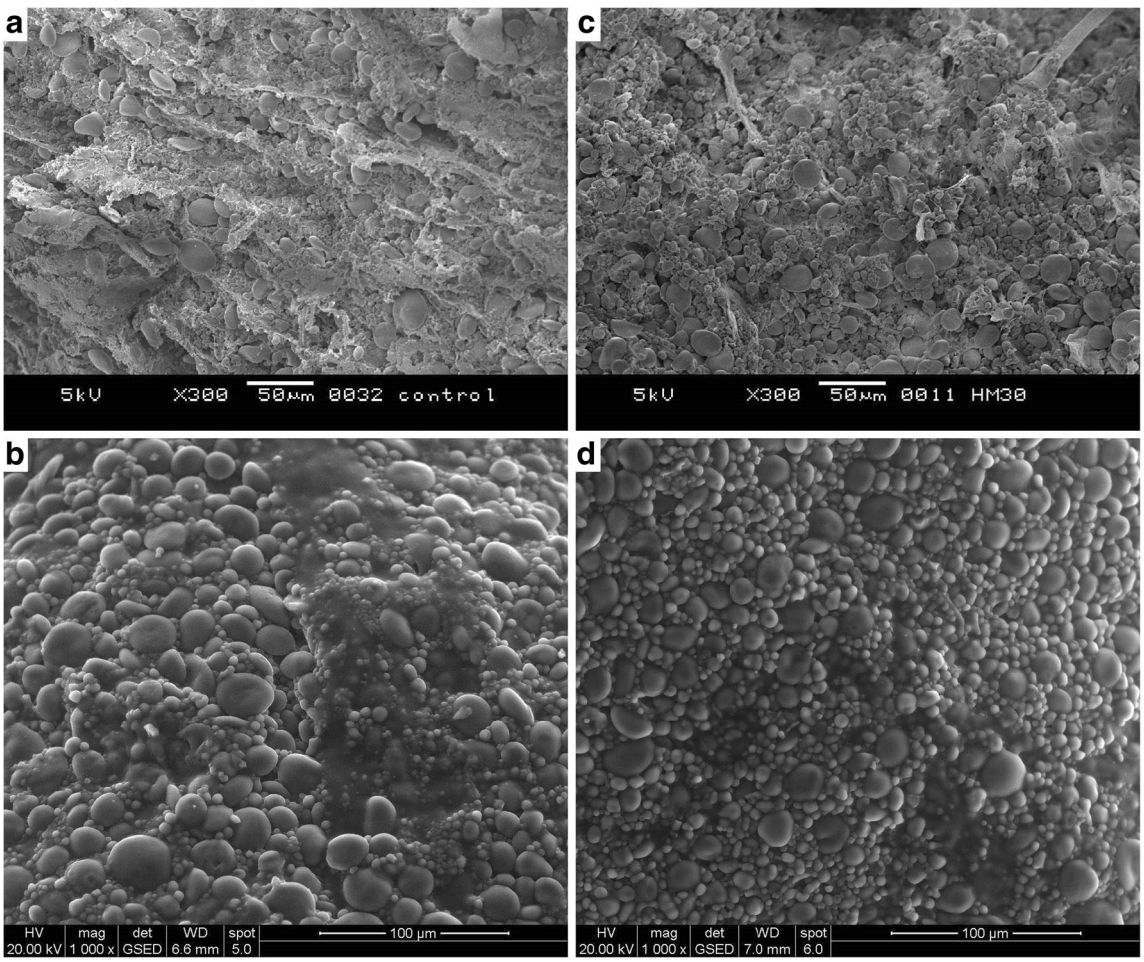

Fig. 4 SEM and ESEM micrographs of doughs. **a** SEM micrograph of control at 300×; **b** ESEM micrograph of control at 1000×; **c** SEM micrograph of HM30 at 300×; **d** ESEM micrograph of HM30 at 1000×

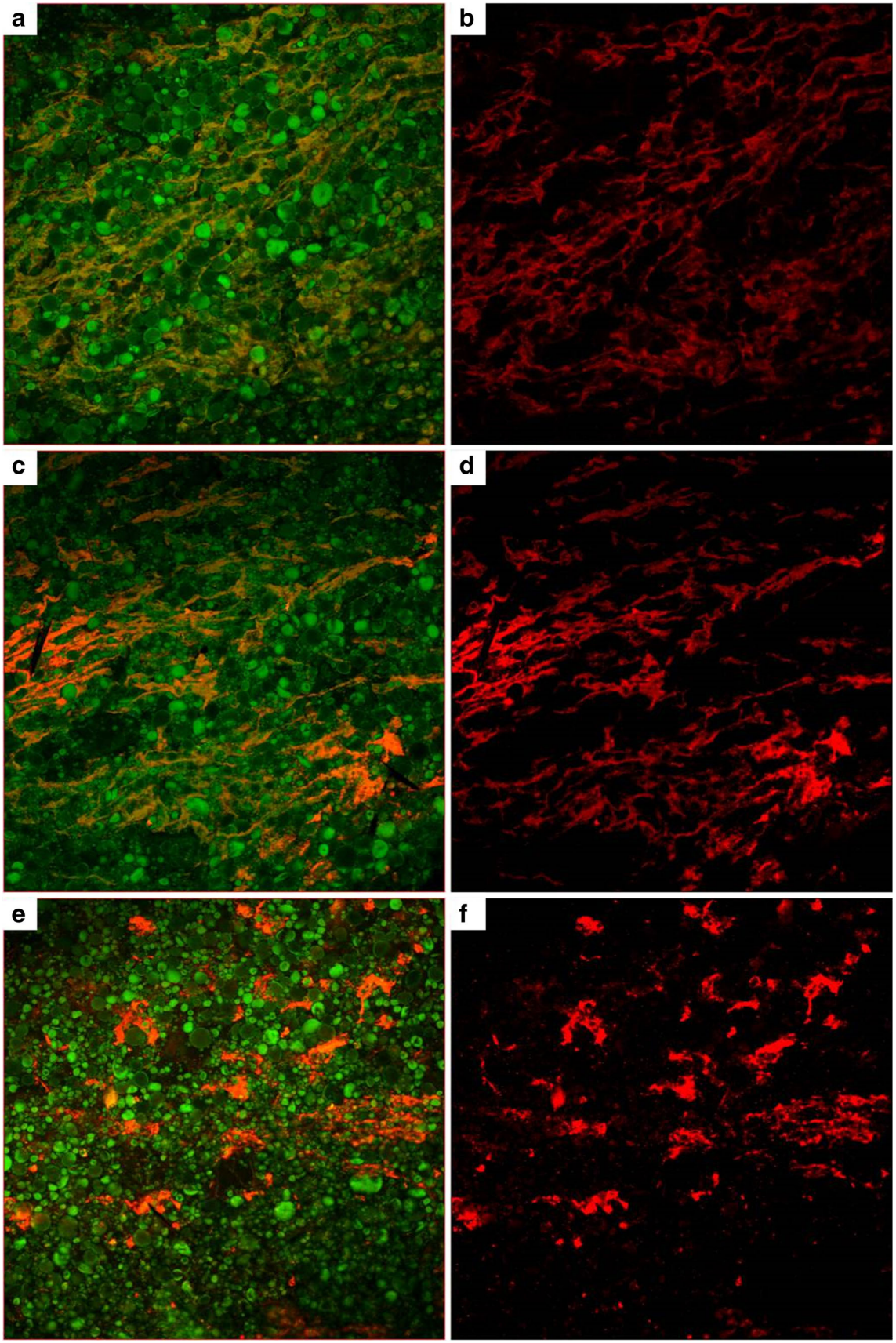
a
b
c
d
e
f

◀ **Fig. 5** CSLM micrographs of doughs. **a** Control in FITC and rhodamin B channels; **b** Control in rhodamin B channel; **c** HM10 in FITC and rhodamin B channels; **d** HM10 in rhodamin B channel; **e** HM30 in FITC and rhodamin B channels; and **f** HM30 in rhodamin B channel. All micrographs were taken at 20×

probably due to the lesser amount of gluten. Finally, gumminess values showed the same behavior as hardness since this parameter is calculated as hardness × cohesiveness.

Water Content and Water Mobility

Due to the increase in farinographic water absorption, the doughs presented a progressive and significant increase in moisture content with the increasing concentrations of HM from 43.63 ± 0.07% to 45.12 ± 0.44% for the control and HM30, respectively (wet basis). However, a_w values did not show statistical differences among samples (mean a_w = 0.9790 ± 0.0068).

^{1}H-NMR assays can be used to evaluate the molecular mobility of the system. Decay curves obtained by ^{1}H-NMR were analyzed using an exponential model

$$y = \sum_{i=0}^{n} A_i \times e^{(-x/T_{2i})} \quad (5)$$

where y is the intensity of the signal of protons in the sample (in volts), A_i represents the proportion of ^{1}H in the T_{2i} state (in volts), and T_{2i} is the transversal relaxation time (in milliseconds). All curves fitted very well ($r^2 > 0.97857$) in Eq. 5 with one term ($n = 1$). Since the number of terms is related to the populations of protons with different mobility, these results mean that it was not possible to distinguish more than one population of protons in these samples, which was in agreement with Correa et al. (2014). The doughs showed that A increased progressively from 0.49 ± 0.02 to 0.60 ± 0.01 V when HM replacement increased from 0 to 30%, which could be related to the increasing moisture content. In relation to T_2, all samples with HM exhibited higher values than the control (8.9 ± 0.5 ms), but there were no differences among samples with HM (9.6 ± 0.7 ms). In general, the values of A and T_2 would indicate that samples with HM had more protons with higher mobility. Doona and Baik (2007) studied the spin-spin relaxation times and their dependence on the sample moisture content of wheat doughs and wheat dough model systems prepared with a mixture of water, wheat gluten and wheat starch. They reported two distinguishable populations of protons. The first one, small and located at $T_2 = 0.1$ ms, did not show a strong dependence on the moisture content, the second one being moisture dependent and with T_2 between 3 and 10 ms according to the increasing water content. The behavior of the only proton population found in the present study is in accordance with the second population observed by Doona and Baik (2007).

In conclusion, mixes of wheat flour and HM exhibited doughs with higher moisture and water mobility.

Microstructural Analysis

Particle Size Profile

The volume weighted distributions for WF and HM starches are depicted in Fig. 3a. These distributions showed a tetramodal pattern for WF starch (peaks at 1.10, 3.31, 22.91, and 158.49 μm) and a trimodal pattern for HM starch (peaks at 1.44, 11.48, and 79.43 μm). The characteristic parameters of the size distribution analysis: D[4,3], D(0.1), D(0.5), and D(0.9) and specific surface area are summarized in Table 5. The volume moment mean D[4,3] shows that HM starch granules were smaller than wheat flour starch granules. In the same sense, the D(0.9) percentile value indicated that with a maximum diameter of 22.98 μm, 90% of the sample volume is obtained, while in the case of wheat flour the maximum starch diameter below which 50% of the sample volume exists was 20.56 μm. Thus, the percentile values showed that for HM most of the starch granules diameters were between 4.26 and 22.98 μm, while for wheat flour they were between 3.65 and 46.0 μm. These results led to a higher specific surface area for HM than for WF granules.

The WF starch pattern distribution obtained here is in agreement with the results previously reported by Xu et al. (2016) for starches from different wheat cultivars.

Using the volume distribution of WF and HM starches, the corresponding theoretical distribution for the premixes was calculated taking into account the respective proportions of WF and HM. This theoretical volume distribution (Fig. 3b) suggests that the substitution of WF for HM would lead to a progressive displacement of the main peaks to lower sizes and also to a decrease in the peaks at 3.31, 22.91, and 158.49 μm, with a small increment in the peak at 1.10 μm.

As expected, in the premixes the substitution of wheat flour by HM would produce a narrow volume distribution, a lower D[4,3] and an increase of specific surface area (Table 5). Thus, the principal effect of the use of HM in the premix formulations would be the increase in the number of starch granules with smaller sizes. This effect could partially explain the increase in the farinographic water absorption values obtained at increasing levels of HM due to the higher exposed surface area of the starch, which would bind more water.

Dough Microscopy

Images of the doughs were acquired with SEM and ESEM microscopes at 300× and 1000×, respectively (Fig. 4). SEM revealed the presence of a well-developed gluten network with starch granules embedded in the control dough (Fig. 4a). Besides, the control sample exhibited gluten strands and

Table 6 Pearson's more relevant correlation coefficients

	WA	DT	S	WaRC	LARC	GPI	W G	D G	*G'* log *a*	*G' n*	Hard.	Resil.	Moist.	*A*	T_2	*FD*
WA		−0.944	−0.9841*	0.989*	−0.9842*	−0.9818*	−0.9821*	−0.9748*	0.9392	−0.9971*	0.9531*	−0.9914*	0.9971*	0.9799*	0.8819	−0.8199
DT	−0.944		0.9843*	−0.8848	0.9843*	0.9774*	0.9837*	0.9896*	−0.7881	0.9314	−0.8384	0.957*	−0.9661*	−0.9626*	−0.943	0.9517*
S	−0.9841*	0.9843*		−0.9486	0.9933*	0.9854*	0.9908*	0.9902*	−0.8643	0.9721*	−0.8928	0.9797*	−0.9943*	−0.9738*	−0.9435	0.9086
WaRC	0.989*	−0.8848	−0.9486		−0.9485	−0.9482	−0.9459	−0.933	0.9727*	−0.9904*	0.9697*	−0.9708*	0.975*	0.952*	0.8232	−0.7316
LARC	−0.9842*	0.9843*	0.9933*	−0.9485		0.9984*	0.9998*	0.9989*	−0.8842	0.9804*	−0.9207	0.993*	−0.9936*	−0.9929*	−0.9049	0.8859
GPI	−0.9818*	0.9774*	0.9854*	−0.9482	0.9984*		0.9992*	0.9976*	−0.8955	0.9823*	−0.9341	0.996*	−0.9898*	−0.9979*	−0.88	0.8657
W G	−0.9821*	0.9837*	0.9908*	−0.9459	0.9998*	0.9992*		0.9992*	−0.8845	0.9796*	−0.9227	0.9935*	−0.9917*	−0.9946*	−0.8979	0.8826
D G	−0.9748*	0.9896*	0.9902*	−0.933	0.9989*	0.9976*	0.9992*		−0.8656	0.971*	−0.9079	0.9884*	−0.9874*	−0.9913*	−0.9054	0.898
G' log *a*	0.9392	−0.7881	−0.8643	0.9727*	−0.8842	−0.8955	−0.8845	−0.8656		−0.9573*	0.9912*	−0.9314	0.9128	0.9142	0.672	−0.5764
G' n	−0.9971*	0.9314	0.9721*	−0.9904*	0.9804*	0.9823*	0.9796*	0.971*	−0.9573*		−0.9726*	0.9946*	−0.9915*	−0.9852*	−0.8461	0.7879
Hard.	0.9531*	−0.8384	−0.8928	0.9697*	−0.9207	−0.9341	−0.9227	−0.9079	0.9912*	−0.9726*		−0.9603*	0.9347	0.9519*	0.6991	−0.635
Resil.	−0.9914*	0.957*	0.9797*	−0.9708*	0.993*	0.996*	0.9935*	0.9884*	−0.9314	0.9946*	−0.9603*		−0.9926*	−0.9975*	−0.8578	0.8252
Moist.	0.9971*	−0.9661*	−0.9943*	0.975*	−0.9936*	−0.9898*	−0.9917*	−0.9874*	0.9128	−0.9915*	0.9347	−0.9926*		0.9845*	0.9069	−0.8595
A	0.9799*	−0.9626*	−0.9738*	0.952*	−0.9929*	−0.9979*	−0.9946*	−0.9913*	0.9142	−0.9852*	0.9519*	−0.9975*	0.9845*		0.8479	−0.8329
T_2	0.8819	−0.943	−0.9435	0.8232	−0.9049	−0.88	−0.8979	−0.9054	0.672	−0.8461	0.6991	−0.8578	0.9069	0.8479		−0.9678*
FD	−0.8199	0.9517*	0.9086	−0.7316	0.8859	0.8657	0.8826	0.898	−0.5764	0.7879	−0.635	0.8252	−0.8595	−0.8329	−0.9678*	

*$p < 0.05$, significant correlation

G' log a, intercept of the modeled curves for *G'*; *G' n*, slope of the modeled curves for *G'*; Hard., hardness; Resil., resilience; Moist., moisture. For the other abbreviations see the text

gluten films. On the other hand, ESEM micrographs of this sample (Fig. 4b) showed a predominant presence of starch granules, although they could be seen embedded in a structure associated with the gluten matrix. In ESEM microscopy, samples are not dehydrated for the observation. So, the structures identified as gluten appeared as smooth, soft and transparent lamellae.

In HM30 SEM and ESEM images, a higher proportion of smaller starch granules were observed, but a well-formed gluten network was not evident (Fig. 4c, d). The greater number of starch granules of smaller size (see "Particle Size Profile") would lead to a better packing capacity of the solid particles, since the interstitial spaces between the larger starch granules are filled by the smaller ones, as reported by other authors (Rueda et al. 2016), forming a more compact structure.

Confocal scanning laser microscopy (CSLM) images of doughs dyed with FITC and rhodamine B at 20× were obtained (Fig. 5). The micrographs showed that samples had different arrangements of the gluten network, which can be seen in more detail in the micrographs of the rhodamine B channel (Fig. 5b–f). The control and HM10 doughs exhibited well cross-linked and orientated networks (Fig. 5a–d). However, the protein arrangement shown in HM30 sample was discontinuous, indicating a poorly developed network (Fig. 5e, f). The high concentration of smaller starch granules and the decrease in the amount of gluten proteins, due to the gluten dilution effect, would be responsible for a hindered development of the network. Conformational differences in the gluten arrangement of the samples could be quantitatively analyzed by extracting the fractal dimension (*FD*) parameter from Eq. 4. *FD* reflects the complexity of a matrix; a decrease in this parameter in HM dough would reveal the lesser development of the gluten network. It is noticeable that *FD* decreased significantly with the use of HM. The *FD* values obtained were 1.50 ± 0.07, 1.35 ± 0.09, 1.21 ± 0.09, and 1.28 ± 0.12 for the control, HM10, HM20, and HM30, respectively. However, no statistical differences were found between HM20 and HM30.

These microstructural modifications could in part explain the changes observed in the small amplitude rheology assays for HM30 and would be in agreement with the filler-matrix composite model.

Correlations

The Pearson's correlation analysis was performed in order to find significant relationships among the parameters obtained by the different assays. A positive correlation was found between the farinographic parameter WA and both the ^{1}H-NMR parameter A and the SRC parameter WaRC, while the SRC values related to the glutenin content of the samples, LARC and GPI, correlated negatively with them. Besides, a negative correlation was found between WA and wet and dry gluten, showing that in the HM doughs the higher absorption of water was strongly ruled by the increased starchy fraction (Table 6).

As expected, the values of farinographic parameters DT and S had a strong and positive correlation with both the wet and the dry gluten values. In addition, the fractal dimension parameter *FD* correlated positively with DT. This suggests that a lesser amount of gluten in HM doughs would develop in less time and in a less complex way. This would be confirmed by the positive correlation between LARC and GPI with respect to the DT, S and wet and dry gluten values. Additionally, hardness positively correlated with WA, WaRC, and *A*, while the slope (*n*) of the modeled curves for G' correlated negatively with these three parameters. Thus, the increasing population of the starch particles would lead to higher water absorption and mobility, and an increment of the solid-like behavior of doughs (Table 6).

Conclusions

All the premixes formulated with HM led to the production of doughs with good handling characteristics, which would be able to go through a breadmaking process. The effect of the replacement of WF by HM on the premixes changed the water requirements for the formation of the doughs. Moreover, the use of increasing HM concentrations, with the consequent decrease in the gluten content, leads not only to an increase of water absorption but also to an increase in the hardness and the elastic behavior of the doughs. These effects were especially marked at higher levels of replacement. Nevertheless, HM20 dough presented appropriate rheological characteristics. So, this level of replacement would be adequate for obtaining fiber-enriched breads.

The mechanisms involved in the changes of the dough characteristics would be related to the gluten dilution effect and the modification of the starch particle size profiles of the doughs, both produced by the replacement methodology. As the starch granules from HM have a smaller particle size distribution and can fill the interstitial spaces between the larger granules of WF, a more compact matrix is obtained. However, these mechanisms would not explain the particular rheological and microstructural effects observed for HM30. The filler-matrix composite model would provide an approach to the characterization of this sample even though the gluten does not form an isotropic network. Further experiments must be done to confirm the usefulness of this model for these systems.

Acknowledgements The authors want to thank Ingredion Baradero S.A. for the donation of the Hi-Maize starch for the experiences.

Funding Information The research was done with funds of the Universidad Nacional de La Plata (project UNLP 11X/661), the Agencia Nacional de Promoción Científica y Tecnológica (PICT2013-

0007) and the Consejo Nacional de Investigaciones Científicas y Técnicas (PIP CONICET 0289).

References

AACC International. (2000a). Farinograph method for flour 54-21.01. In: AACC International approved methods (pp. 1–7). AACC International.

AACC International. (2000b). Solvent retention capacity profile 56-11.02. In: AACC International approved methods (pp. 1–2). AACC International.

Ahmed, J., Almusallam, A. S., Al-Salman, F., AbdulRahman, M. H., & Al-Salem, E. (2013). Rheological properties of water insoluble date fiber incorporated wheat flour dough. *LWT-Food Science and Technology, 51*(2), 409–416.

Aigster, A., Duncan, S. E., Conforti, F. D., & Barbeau, W. E. (2011). Physicochemical properties and sensory attributes of resistant starch-supplemented granola bars and cereals. *LWT-Food Science and Technology, 44*(10), 2159–2165.

Alfa, M. J., Strang, D., Tappia, P. S., Graham, M., Van Domselaar, G., Forbes, J. D., et al. (2017). A randomized trial to determine the impact of a digestion resistant starch composition on the gut microbiome in older and mid-age adults. *Clinical Nutrition.*

Almeida, E. L., Chang, Y. K., & Steel, C. J. (2013a). Dietary fibre sources in frozen part-baked bread: Influence on technological quality. *LWT-Food Science and Technology, 53*(1), 262–270.

Almeida, E. L., Chang, Y. K., & Steel, C. J. (2013b). Dietary fibre sources in bread: Influence on technological quality. *LWT-Food Science and Technology, 50*(2), 545–553.

Altuna, L., Ribotta, P. D., & Tadini, C. C. (2015). Effect of a combination of enzymes on dough rheology and physical and sensory properties of bread enriched with resistant starch. *LWT-Food Science and Technology, 64*(2), 867–873.

Altuna, L., Ribotta, P. D., & Tadini, C. C. (2016). Effect of a combination of enzymes on the fundamental rheological behavior of bread dough enriched with resistant starch. *LWT-Food Science and Technology, 73*, 267–273.

Aravind, N., Sissons, M., Fellows, C. M., Blazek, J., & Gilbert, E. P. (2013). Optimisation of resistant starch II and III levels in durum wheat pasta to reduce in vitro digestibility while maintaining processing and sensory characteristics. *Food Chemistry, 136*(2), 1100–1109.

Arp, C. G., Correa, M. J., Zuleta, Á., & Ferrero, C. (2017). Techno-functional properties of wheat flour-resistant starch mixtures applied to breadmaking. *International Journal of Food Science and Technology, 52*(2), 550–558.

Asp, N. G. (1992). Resistant starch. Proceedings from the second plenary meeting of EURESTA: European FLAIR concerted action on physiological implications of the consumption of resistant starch in man. Preface. *European Journal of Clinical Nutrition, 46*, S1.

Baixauli, R., Sanz, T., Salvador, A., & Fiszman, S. M. (2008). Muffins with resistant starch: Baking performance in relation to the rheological properties of the batter. *Journal of Cereal Science, 47*(3), 502–509.

Bigne, F., Puppo, M. C., & Ferrero, C. (2016). Rheological and microstructure characterization of composite dough with wheat and mesquite (*Prosopis* spp) flours. *International Journal of Food Properties, 19*(2), 243–256.

Brennan, M. A., Monro, J. A., & Brennan, C. S. (2008). Effect of inclusion of soluble and insoluble fibres into extruded breakfast cereal products made with reverse screw configuration. *International Journal of Food Science and Technology, 43*(12), 2278–2288.

Bustos, M. C., Perez, G. T., & León, A. E. (2011). Sensory and nutritional attributes of fibre-enriched pasta. *LWT-Food Science and Technology, 44*(6), 1429–1434. https://doi.org/10.1016/j.lwt.2011.02.002.

Correa, M. J., Añón, M. C., Pérez, G. T., & Ferrero, C. (2010). Effect of modified celluloses on dough rheology and microstructure. *Food Research International, 43*(3), 780–787.

Correa, M. J., Ferrer, E., Añón, M. C., & Ferrero, C. (2014). Interaction of modified celluloses and pectins with gluten proteins. Food Hydrocolloids, 35(0), 91–99.

Dhingra, S., & Jood, S. (2004). Effect of flour blending on functional, baking and organoleptic characteristics of bread. *International Journal of Food Science and Technology, 39*(2), 213–222.

Doona, C. J., & Baik, M.-Y. (2007). Molecular mobility in model dough systems studied by time-domain nuclear magnetic resonance spectroscopy. *Journal of Cereal Science, 45*(3), 257–262.

Fuentes-Zaragoza, E., Riquelme-Navarrete, M. J. J., Sánchez-Zapata, E., & Pérez-Álvarez, J. A. (2010). Resistant starch as functional ingredient: a review. *Food Research International, 43*(4), 931–942.

Genovese, D. B. (2012). Shear rheology of hard-sphere, dispersed, and aggregated suspensions, and filler-matrix composites. *Advances in Colloid and Interface Science, 171–172*, 1–16.

Grabitske, H. A., & Slavin, J. L. (2009). Gastrointestinal effects of low-digestible carbohydrates. *Critical Reviews in Food Science and Nutrition, 49*(4), 327–360.

Hasjim, J., Ai, Y., & Jane, J. (2013). Novel applications of amylose-lipid complex as resistant starch type 5. In Y. C. Shi & C. C. Maningat (Eds.), *Resistant starch sources, applications and health benefits* (pp. 79–94). Chichester: John Wiley and Sons Ltd..

Keenan, M. J., Zhou, J., McCutcheon, K. L., Raggio, A. M., Bateman, H. G., Todd, E., Jones, C. K., Tulley, R. T., Melton, S., Martin, R. J., & Hegsted, M. (2006). Effects of resistant starch, a non-digestible fermentable fiber, on reducing body fat. *Obesity (Silver Spring, Md.), 14*(9), 1523–1534.

Korus, J., Witczak, M., Ziobro, R., & Juszczak, L. (2009). The impact of resistant starch on characteristics of gluten-free dough and bread. *Food Hydrocolloids, 23*(3), 988–995.

Kweon, M., Slade, L., & Levine, H. (2011). Solvent retention capacity (SRC) testing of wheat flour: Principles and value in predicting flour functionality in different wheat-based food processes and in wheat breeding—a review. *Cereal Chemistry Journal, 88*(6), 537–552.

Nugent, A. P. (2005). Health properties of resistant starch. *Nutrition Bulletin, 30*(1), 27–54.

Rueda, M. M., Auscher, M.-C., Fulchiron, R., Périé, T., Martin, G., Sonntag, P., & Cassagnau, P. (2016). Rheology and applications of highly filled polymers: a review of current understanding. *Progress in Polymer Science, 66*, 22–53.

Sabanis, D., & Tzia, C. (2009). Effect of rice, corn and soy flour addition on characteristics of bread produced from different wheat cultivars. *Food and Bioprocess Technology, 2*(1), 68–79.

Salinas, M., Carbas, B., Brites, C., & Puppo, M. (2015). Influence of different carob fruit flours (Ceratonia siliqua L.) on wheat dough performance and bread quality. *Food and Bioprocess Technology, 8*(7), 1561–1570.

Sanchez, D. B. O., Puppo, M. C., Añon, M. C., Ribotta, P. D., León, A. E., & Tadini, C. C. (2014). Effect of maize resistant starch and transglutaminase: a study of fundamental and empirical rheology properties of pan bread dough. *Food and Bioprocess Technology, 7*(10), 2865–2876.

Scholz-Ahrens, K. E., Ade, P., Marten, B., Weber, P., Timm, W., Açil, Y., et al. (2007). Prebiotics, probiotics, and synbiotics affect mineral absorption, bone mineral content, and bone structure. *The Journal of Nutrition, 137*(3 Suppl 2), 838S–846S.

Singh, J., Kaur, L., & McCarthy, O. J. (2007). Factors influencing the physico-chemical, morphological, thermal and rheological properties of some chemically modified starches for food applications—a review. *Food Hydrocolloids, 21*(1), 1–22.

Topping, D. L., Fukushima, M., & Bird, A. R. (2003). Resistant starch as a prebiotic and synbiotic: state of the art. *Proceedings of the Nutrition Society, 62*(1), 171–176.

Tsatsaragkou, K., Papantoniou, M., & Mandala, I. (2015). Rheological, physical, and sensory attributes of gluten-free rice cakes containing resistant starch. *Journal of Food Science, 80*(2), E341–E348.

Ukai, T., Matsumura, Y., & Urade, R. (2008). Disaggregation and Reaggregation of gluten proteins by sodium chloride. *Journal of Agricultural and Food Chemistry, 56*(3), 1122–1130.

Xu, Y., Qiu, M., Li, Y., Qian, X., Gu, J., & Yang, J. (2016). Polyamines mediate the effect of post-anthesis soil drying on starch granule size distribution in wheat kernels. *The Crop Journal, 4*(6), 444–458.

Yeo, L. L., & Seib, P. A. (2009). White pan bread and sugar-snap cookies containing wheat starch phosphate, a cross-linked resistant starch. *Cereal Chemistry, 86*(2), 210–220.